VSP VECTOR WAVE FIELD SYNTHESIZING AND SEPARATION TECHNOLOGY BASED ON TIME-VARYING POLARIZATION CHARACTERISTICS

YE LIU[1], GUANGMING ZHU[2], LIFA ZHOU[1] and CHAO GUO[3]

[1] *Department of Geology, Northwest University, Xi'an, 710075 P.R. China.*
[2] *College of Geology Engineering and Geomatics, Chang'an University, Xi'an, 710054 P.R. China.*
[3] *Shaanxi Yanchang Petroleum Corporation, Xi'an, 710075 P.R. China.*
heitongsa@hotmail.com

(Received March 13, 2012; revised version accepted August 8, 2012)

ABSTRACT

Liu, Y., Zhu, G., Zhou, L. and Guo, C., 2012. VSP vector wave field synthesizing and separation technology based on time-varying polarization characteristics. *Journal of Seismic Exploration*, 21: 301-322.

We developed a new time-varying polarization characteristic method for estimating the polarization information from multi-component array VSP data based on the velocity model, covariance matrix analysis and quasi-Newton optimal algorithm. The utilization of both the velocity model and the covariance matrix, which provide an initial value and constraints for the quasi-Newton optimal algorithm as well as the identification of wave field event conditions, enhances the efficiency and the reliability of the algorithm. Effects of both the random noise and the initial value are fully evaluated. Numerical and practical results show that the presented method is reliable and effective.

KEY WORDS: VSP, polarization characteristic, wave field separation, vector wave field.

INTRODUCTION

A Seismogram is the result of interference and superposition of multi-seismic events with different properties, such as polarization angle, amplitude and velocity. Since traditional seismic prospecting methods normally use single vertical component data, which record the projection of vector wave fields (i.e., the scalar wave filed) for seismic processing and interpretation, it

0963-0651/12/$5.00

may cause a significant loss of the waveform information. Only multi-component array systems can fully record the whole wave field from underground. For the unique geometry layout of the borehole seismic, the VSP (vertical seismic profile), the multi-component acquisition system is widely applied. Therefore, the polarization characteristic technology as an important multi-component seismic processing method shows significant effort for borehole seismic, especially for VSP. Compared to surface seismic methods, the polarization technique has better development prospects in the borehole seismic, where multi-component acquisition systems are widely used. Furthermore, the borehole seismic has other advantages over surface seismic methods, such as high SNR (signal to noise ratio) and no receiving Rayleigh waves, which shows an elliptical polarization and causes seismic signals to become polychromatic transients. Consequently, the polarization characteristic in borehole seismic is only associated with linearly polarized waves, such as random noise and body waves.

A conventional VSP polarization characteristic method only evaluates the polarization of the first arrival P-wave and it is assumed that the polarization angle of the S-wave is orthogonal to the P-wave. Then the polarization angles of two events can be achieved for each trace. Ignoring the fact that polarization is time varying, the conventional method can hardly get accurate polarization information for seismic events except for the first arrival P-wave. The conventional method faces much more challenges that are difficult to overcome. Therefore, a time-varying based polarization characteristic technique is needed for borehole seismic. Moreover, accurate polarization angle can help us to achieve the separation of P- and S-vector wave field, which can solve many difficult problems confronted by velocity filtering methods.

Polarization analyses in the surface seismic prospecting have been used for a long time (Lilly and Park, 1995; Reading et al., 2001; Samson, 1983; De Franco, 2001). Most techniques are based on an eigenanalysis of the data covariance matrix constructed in the time or frequency domain (e.g., Samson, 1983; Li, 1994). Rotation of the tri-axial data into the eigenvector frame is called the principal-component transformation and can be obtained directly by using the singular-value decomposition (SVD) of the data matrix (Jackson et al. 1991). Cho and Spencer (1992) developed an algorithm for estimating both the polarization and the velocity in mixed fields based on the least-square error estimation. The algorithm is dependent of the selection of the analysis window, which is subject to dominant periods, SNR and signal durations. Cui (1994) presented a model-based method for determining the VSP polarization angle by using a velocity model and a ray tracing method. Methods for deriving polarization attributes fall into two categories: signal analysis-based methods and model-based methods. The signal analysis-based methods are limited to cases where some complex events and random noises lie within a given time window. And the model-based methods are subject to the accuracy of the model.

In this paper, we present a new method for obtaining polarization attributes and carrying out the separation of P- and S-vector wave fields from multi-component array VSP data. Our method combines the advantages of two categories of methods mentioned above, which may improve both the accuracy and the efficiency of polarization characteristics. Numerical tests show that the presented method is insensitive to the deviation of the optimal initial value and random noises. The synthesis and practical seismic examples illustrate that the method is more accurate and reliable than other exiting methods.

METHODOLOGY

Time-varying polarization characteristic

With the polarization characteristic processing, multi-component seismic vector wave field can be synthesized from scalar wave fields, which can fundamentally solve many problems caused by scalar wave fields.

The first arrival P-wave of the VSP has many advantageous properties, such as high energy, high SNR and rarely presenting complex events within time windows. Hence, conventional VSP polarization characteristic methods normally use the first arrival P-wave. However, these methods ignore the fact that the polarization is varying with time change. From Fig. 1, one can see that the incidence angles of reflection waves at different depths are obviously different. Therefore, time-varying factor has to be taken into account when developing polarization characteristic techniques.

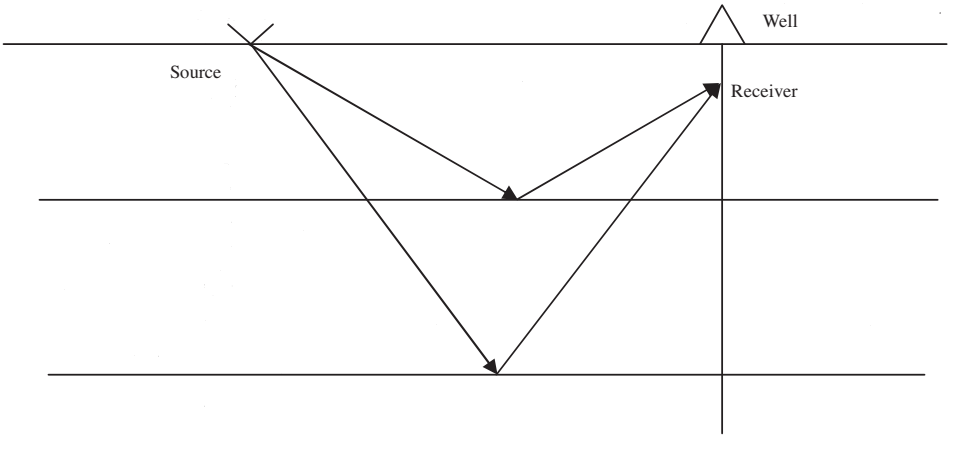

Fig. 1. Different polarizations of reflected waves from different layers in the VSP.

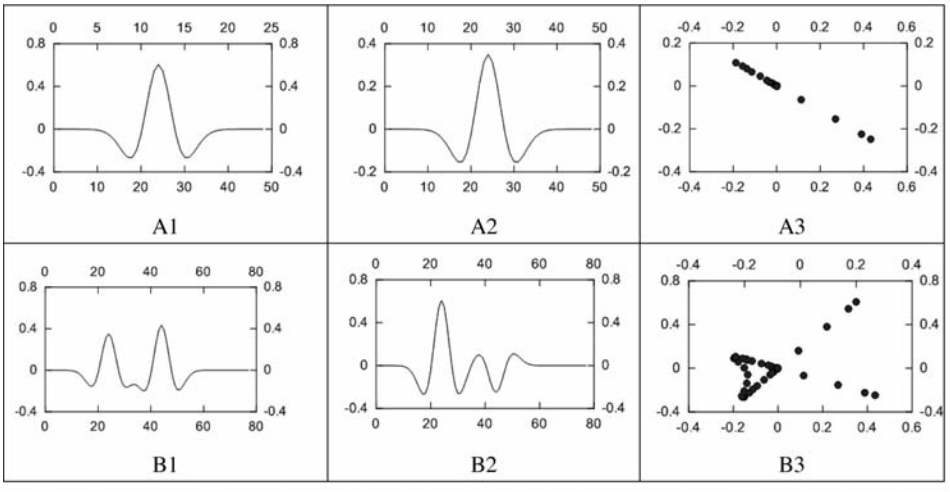

Fig. 2. Seismograms and corresponding hodographs. A: Single wave fields; B: Mixed wave fields; 1: Vertical component; 2: Horizontal component; 3: Hodographs.

Fig. 2 shows seismograms and corresponding hodographs of single and mixed events located within a time window. For the single event condition, the polarization characteristic is very simple and the hodograph exhibits a straight line as shown in Fig. 2 (A3). For the mixed event condition, however, the hodograph doesn't exhibit a straight line anymore and the polarization characteristic becomes much more complicated, as shown in Fig. 2 (B3).

Theoretical basis of the mixed wave field polarization characteristic

The theoretical basis of the presented algorithm is summarized here, the reader are kindly requested to refer to Cho and Spencer (1992) for more details.

We assume that m+1 measurement points are equally spaced with the unit interval within the spatial window, and the first geophone among the m+1 geophones is referred to the n-th geophone in the entire vertical array.

The displacements $U_i^{(n)}(f)$ at the n-th geophone in the frequency domain can be expressed as

$$\begin{Bmatrix} U_3^{(n)}(f) \\ U_1^{(n)}(f) \end{Bmatrix} = \begin{bmatrix} a_3^P & a_3^S \\ a_1^P & a_1^S \end{bmatrix} \begin{Bmatrix} W^P(f) \\ W^S(f) \end{Bmatrix} , \quad (1)$$

where the a_i^α indicates the *i-directional* component of the polarization vector of the α-wave, and $W^\alpha(f)$ indicates the waveform of the α-wave, α is used for identifying the event condition (P or S), and the subscript i is used for identifying the direction of a vector component, that is vertical (i = 1) or horizontal (i = 3).

From eq. (1), we have

$$\begin{Bmatrix} W^P(f) \\ W^S(f) \end{Bmatrix} = \begin{bmatrix} a_3^P & a_3^S \\ a_1^P & a_1^S \end{bmatrix}^{-1} \times \begin{Bmatrix} U_3^{(n)}(f) \\ U_1^{(n)}(f) \end{Bmatrix} . \tag{2}$$

When the α-wave field is non-dispersive, the phase difference between the scalar spectrum of the α-wave recorded at the n-th geophone and that recorded at the (n+1)-th geophone becomes a linear function of frequency due to a phase difference of the waveform.

The amplitude of the α-wave at the (n+1)-th geophone may be expressed by multiplying the amplitude at the n-th geophone with the scaling factor g_α. Thus the Fourier spectrum of the waveform at the (n+1)-th geophone is written

$$\begin{Bmatrix} U_3^{(n+1)}(f) \\ U_1^{(n+1)}(f) \end{Bmatrix} = \begin{bmatrix} a_3^P & a_3^S \\ a_1^P & a_1^S \end{bmatrix} \begin{bmatrix} g_P e^{j\phi_P} & 0 \\ 0 & g_S e^{j\phi_S} \end{bmatrix} \begin{bmatrix} a_3^P & a_3^S \\ a_1^P & a_1^S \end{bmatrix}^{-1} \times \begin{Bmatrix} U_3^{(n)}(f) \\ U_1^{(n)}(f) \end{Bmatrix} . \tag{3}$$

where $\phi_P = 2\pi f q^P \Delta$ and $\phi_S = 2\pi f q^S \Delta$ are the linear phase difference between the two observations of the P-wave and the S-wave, respectively, and q^α is the slowness of the α-wave.

Assuming

$$A = \begin{bmatrix} a_3^P & a_3^S \\ a_1^P & a_1^S \end{bmatrix} , \quad \Lambda = \begin{bmatrix} g_P e^{j2\pi f q^P \Delta} & 0 \\ 0 & g_S e^{j2\pi f q^S \Delta} \end{bmatrix} . \tag{4}$$

From eqs. (2) and (3), we can get the relation between the Fourier spectra of two adjacent points as follows

$$U^{(n+1)} = Y U^{(n)} , \tag{5}$$

where $Y = A \Lambda A^{-1}$ and A^{-1} denotes the inverse of the matrix A. The matrix is invertible since the P and S polarization vectors are not collinear.

As we know, body waves are regular and the noise is random. Thus the transfer matrix Y could be obtained by solving the following equation

$$\| U^{(n+1)} - YU^{(n)} \| = \textit{Minimum} \quad , \tag{6}$$

with the quasi-Newton optimal algorithm. Eq. (6) may be written as

$$\begin{bmatrix} U_{11}^{(n+1)} \\ U_{21}^{(n+1)} \end{bmatrix} - \begin{bmatrix} Y_{11} & Y_{12} \\ Y_{21} & Y_{22} \end{bmatrix} \times \begin{bmatrix} U_{11}^{(n)} \\ U_{21}^{(n)} \end{bmatrix} = E \quad , \tag{7}$$

where $E_{11} = U_{11}^{(n+1)} - Y_{11} \times U_{11}^{(n)} - Y_{12} \times U_{21}^{(n)}$ and $E_{21} = U_{21}^{(n+1)} - Y_{11} \times U_{21}^{(n)} - Y_{12} \times U_{22}^{(n)}$. The eigenvalues A of the transfer matrix Y provide the polarization angles for P- and S-waves. Then the vector wave separation can be carried out with the use of eq. (2) and the polarization matrix A.

The presented algorithm in this paper is based on the theory described in Cho and Spencer (1992). The improvements that have been done to the algorithm developed by Cho and Spencer (1992), are as follows: (1) utilization of the quasi-Newton optimal method instead of the least-square error estimation algorithm, resulting in more accurate and reliable polarization attributes; (2) extending the algorithm to VSP, and solving limitations of this algorithm in practical application.

The analysis of polarization characteristic method

Limitation analysis of the algorithm

There are two types of limitations on the algorithm:

1. When implementing the algorithm, it is assumed that there are fewer than two events located within a given time window.

   Since VSP data contain four distinct apparent moveout velocities, e.g., up-going and down-going P and S, it does not meet the assumption of the algorithm above. For this reason, VSP data need to be pre-processed with a velocity filter method for separating up-going and down-going waves. Then we can get up-going and down-going data, respectively, so that the underlying assumption of the algorithm is met.

2. The algorithm is limited to the case where a single event lies within a given time window.

   To test its effect on the algorithm, we designed a numerical experiment of a Ricker wavelet with a 40 Hz central frequency, representing a single event condition with polarization angle of 30°. A polarization angle of

25.7° was obtained, and the error is 4.3° caused by the initial value deviation, which always exists for a single event. The reason is that the single event condition cannot be taken into account in the initial value computation.

There are many techniques which are suitable for the polarization characteristic when a single event presents. In this paper, we utilize the covariance matrix analysis method to identify the wave field event condition (i.e., signal or mixed wave fields) within the time window and to achieve polarization characteristic for signal event condition.

Application of polarization characteristic method

The VSP-wave separation normally uses velocity filters, such as the median and FK filter, depending on the velocity difference between seismic events. These methods are limited to cases where P- and S-waves have close velocities. However, the wave separation with polarization characteristic is more advanced than the velocity filter, the resulting polarization angles of P- and S-wave are always in different quadrants no matter how close of their velocities. Hence, the polarization characteristic can solve many difficult problems confronted by the velocity filter in the wave separation.

A covariance matrix is a statistic method to transform a time signal into an analytic signal. The matrix is determined by sliding data windows to decompose the data into their principal energy components given by eigenvalues and eigenvector pairs. The eigenvalues present the energy components and the eigenvectors present the corresponding principal directions. In this paper, we use the eigenvalue ratio of the matrix to identify the seismic event condition for a time window. In the implementation of this method, we need to set a threshold value which is proportional to the SNR of seismic data. If the ratio of matrix eigenvalues is bigger than the threshold, we can confirm that the condition of a seismic event is mixed, otherwise it is single.

A simple method that measures the length between three zero values of waveform is used to determine the length of time windows, which should not include more than two events and makes it close to wave-length. Moreover, STFT (short-time Fourier transform), which uses Gaussian-shaped windows and keeps the option to stabilize the cross spectra over the frequencies as a TFDF (time-frequency domain filter) method, is used to transform time series signal to time-frequency domain for the algorithm analysis.

A VSP P-wave velocity model can be built by using the first arrival time of P-wave, assuming the velocity of S-wave equals to $P_{velocity} \times 2/3$. With the ray tracing method, we can obtain every ray's incidence angle and the

corresponding arriving time at geophones. Finally, with the linear interpolation method, a polarization angle model can be built for initial values and constraints in the optimal algorithm.

Numerical tests and analysis

Comparison and analysis of the optimal method

We simulated a seismogram with two traces, two components and two Ricker wavelets representing P- and S-waves, respectively, for the numerical test. The central frequency of these waves is 40 Hz, the geophone interval is 10m, the velocities of P- and S-wave are 2000 m/s and 1300 m/s, respectively, the polarization angles of P and S are 30° and −45°, respectively.

In this numerical test, the initial value is given with about 50% deviations, namely, the initial value of P-wave is 15° and that of S-wave is −67°. The results of this numerical test illustrated in Table 1 show that our method is more accurate even with the initial value deviation of 50%, compared to the results obtained by using the covariance matrix analysis (Li, 1994) and the least square error estimation method (Cho and Spencer, 1992).

Table 1. Comparison and analysis of polarization methods.

Seismic event	Covariance matrix	Least square error	Quasi-Newton optimal
P (30°)	21.34°	2.86°	34.88° (15°)
S (−45°)	−68.65°	−55.18°	−44.50° (−67°)

The effect of the errors caused by the initial value deviation is estimated by the equations of $(P' - P)/P$ and $(S' - S)/S$, where P and S represent vector wave fields, respectively, P′ and S′ represent wave separation results with the polarization angle from quasi-Newton optimal algorithm. The estimation results show the error of P is between 0.1% ~ 2.6% and that of S is between 0.8% ~ 2%. If we use the traditional scalar wave field separation method to separate P from the vertical component seismic data and S from the horizontal component data, the error for P is 50% and that for S is 29.29%. Even with the initial value deviation, the vector wave separation results still are more accurate and reliable than those obtained by using the traditional method. Thus, we conclude that the new vector wave separation method can solve many problems confronted by traditional methods.

Identification of seismic event conditions

In this section, we investigate the ability of the eigenvalue ratio of the covariance matrix, which represents the ratio of the energy of events, to identify seismic event conditions. Using the same numerical data as mentioned above, P-wave is multiplied by a coefficient factor q. Table 2 shows the wave event conditions. One can see that the eigenvalue ratio decreases with decreasing q. When q decreases to zero, the eigenvalue ratio becomes zero, too, and the seismic event condition becomes single.

Table 2. Wave event conditions identified with the covariance matrix analysis method.

Q	1	0.8	0.5	0.3	0.1	0.01	0
Eigenvalue ratio	0.7018	0.5531	0.2202	0.0766	0.0080	0.00077543	0
Event condition	mixed	mixed	mixed	mixed	mixed	mixed	single

Numerical experiment analysis for initial values

The following numerical experiments are used to examine effects of initial values on polarization results of the optimal algorithm.

Table 3 illustrates the experiment results. For the first three experiments we use a positive deviation, and for the remaining experiments we use a mixed deviation, i.e., a negative deviation for P and a positive deviation for S. From Table 3, one can see that the P-wave is influenced much more than the S-wave by an initial value deviation. However, note that even with an initial value deviation of 50%, the errors are less than 5°, namely, the method is still reliable.

Table 3. Polarizations with different initial value deviations.

Initial value deviation	0%	10%	20%	30%	40%	50%
P-wave initial value	30°	33°	36°	21°	18°	15°
S-wave initial value	−45°	−40.5°	−36°	−58°	−63°	−67°
Results of P	30°	30.06°	26.75°	34.21°	34.61°	34.88°
Results of S	−45°	−44.66°	−44.55°	−44.50°	−44.50°	−44.50°

Fig. 3 shows the distribution graphs of the polarization characteristic results with an initial value deviation of 50%. The polarization distribution of the S-wave is more stable than that of the P-wave.

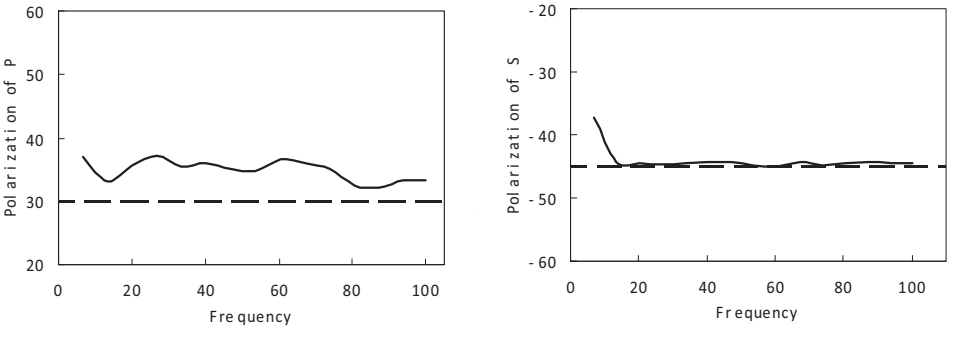

Fig. 3. Polarization characteristic distribution graphs obtained with 50% deviation of initial values. Left: for P-wave ; Right: for S-wave

The stability analysis of the optimal algorithm

Six parameters that completely characterize the properties of two waves include slowness, amplitude change rate and polarization angle. These six parameters are associated with the complex transfer matrix Y. In this section, we discuss the relationship between the polarization angle, the slowness and the transfer matrix Y, which is significant for the stability and reliability of the optimal algorithm.

A numerical test is implemented to investigate the relationship between the polarization angle and all the eight elements of transfer matrix Y. In the test, the velocities of P vary between 1000 m/s and 5000 m/s and that of S is set to be 3000 m/s, the geophone interval is 10 m, polarization angles of P vary between 0°and 180°and the polarization angle of S-wave is set to be 30°. In Fig. 4(1) and Fig. 4(2), the x-axis indicates the polarization angle and the velocity, respectively, and the y-axis indicates transfer matrix parameter values, and the curves A ~ H represent the eight elements of real and imaginary parts of the transfer matrix Y, respectively.

From Fig. 4(1), we can see that the elements of the transfer matrix change smoothly when the polarization of P and S are in different quadrants. There are some abnormal points where the polarization angle of P is close to that of S. When implementing this method, the pre-processing, in which up-going and down-going waves are separated, can make the polarization angle

of P and S always in different quadrants. In addition, and we carried out the similar numerical test with the velocity attribute and the results are shown in Fig. 4(2). The curves have a smooth feature too. This indicates that the optimal algorithm is not sensitive to the seismic event attributes, namely velocity and polarization angles, and it might be very stable when applied to practical data sets.

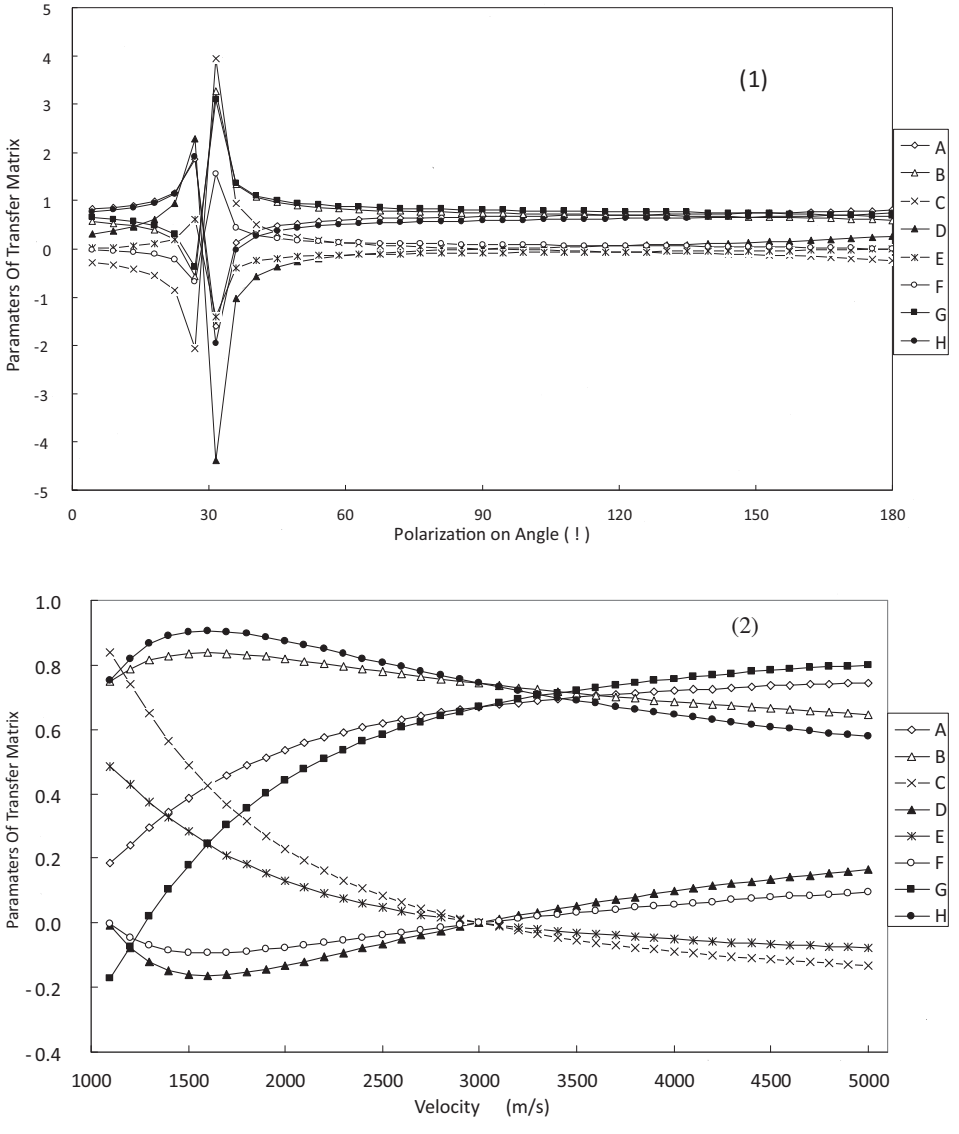

Fig. 4. The distribution of eight elements of the transfer matrix associated with polarization angle (1) and velocity (2) of P-wave: Curves A and B are real and imaginary part of Y(1,1) C and D real and imaginary part of Y(1,2), E and F real and imaginary part of Y(2,1) , and G and H real and imaginary part of Y(2,2), respectively.

Random noise analysis

To test the performance of this technique in the presence of a random noise, we generate four noise curves, as shown in Fig. 5. These four noise curves are multiplied by a factor to fulfill SNR demand, and then they are added to the seismic data.

Table 4 shows the results of random noise tests for different SNRs. In the test, we assume that the initial value of the optimal algorithm does not have any deviation. Note that the accuracy of the polarization is proportional to the SNR. If the SNR is greater than 10, the results become reliable. Thus, the de-noise processing should be done before the polarization characteristic, and the following wave separation process should be based on the original seismic data with noise, which not only can solve the problems caused by random noises for polarization characteristic, but also can avoid de-noise processing's effect on seismic events.

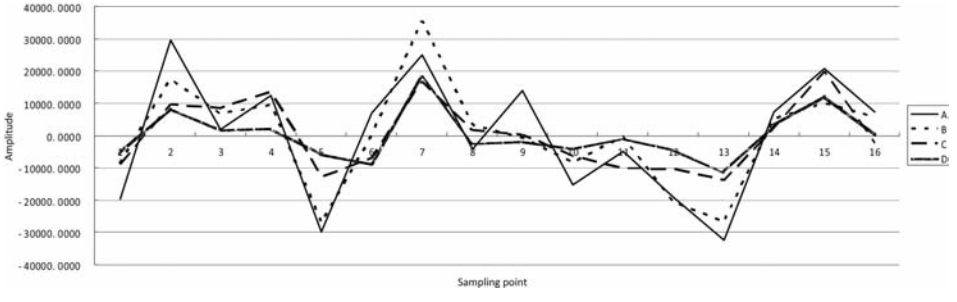

Fig. 5. Random noise. A: Horizontal component, second trace; B: Vertical component, second trace; C: Horizontal component, first trace; D: Vertical component, first trace.

Table 4. Noise analysis.

SNR		8	10	20	30	40
algorithm	P	20.01	25.2	25.3	28.35	29.42
result	S	−35.18	−43.48	−44.45	−44.37	−44.56

APPLICATION

The processing flow we proposed has seven steps:

1. VSP velocity modeling by first arrival time.

2. Computation of polarization for each sample point by a ray tracing method to build a polarization model as an initial value for subsequent processes.

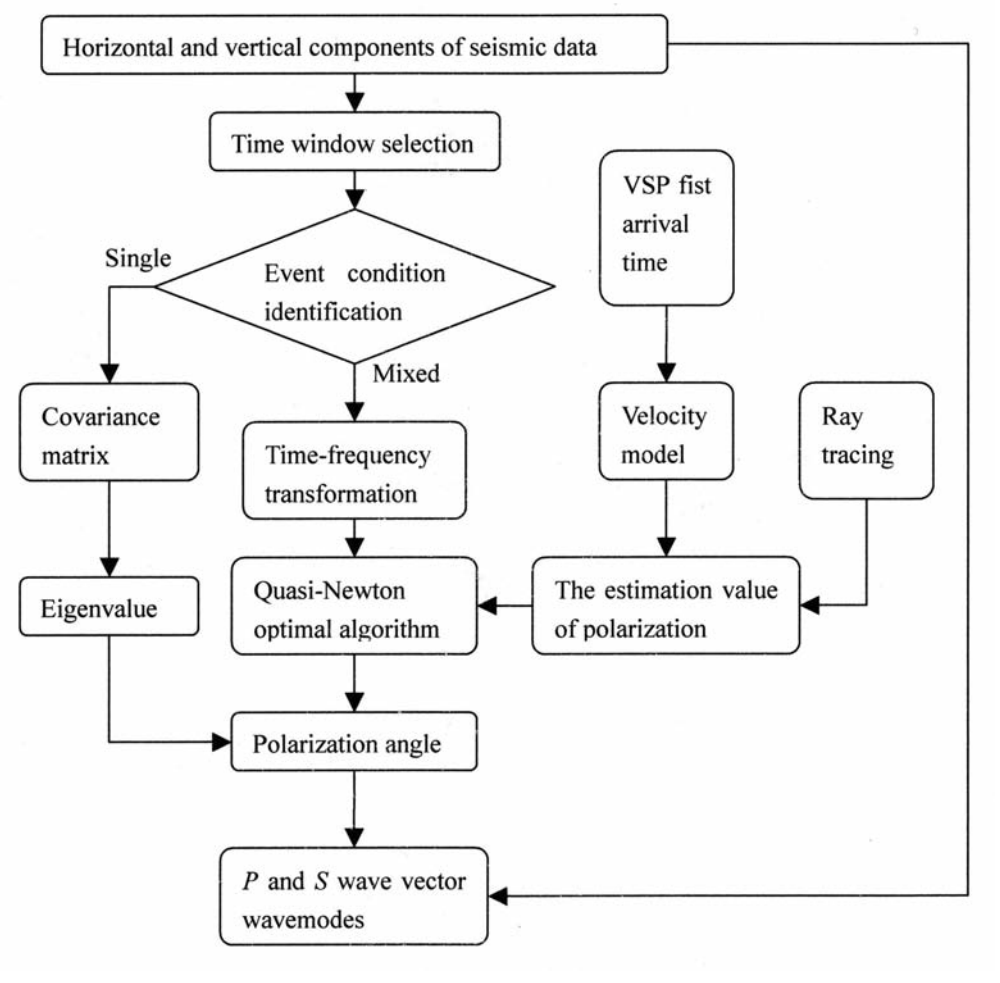

Fig. 6. Flow-diagram of the polarization characteristic processing scheme for multi-component VSP data.

3. Selection of a non-overlapping moving time window.

4. Identification of event conditions for a time window by the covariance matrix. If it's single, the polarization can be directly computed by the eigenvalue of covariance. Otherwise, turn to step 5.

5. Transformation from a time series signal to a time-frequency domain signal with STFT.

6. Computation of the transfer matrix Y with the quasi-Newton optimal algorithm.

7. Separation and synthesis of scalar wave fields into their constituent vector wavemodes with the eigenvalue matrix A from transfer matrix Y [eq. (2)].

SYNTHETIC AND PRACTICAL SEISMIC TEST

Synthetic seismic test

This paper mainly focuses on the up-going wave field which is associated with the main target of VSP processing, and depends if the up-going wave has more complicated interference waves and lower SNR than the down-going wave, which represent most of wave field problems that will be encountered in a practical use of polarization characteristic techniques.

To examine the performance of the technique presented in this paper, a set of the vertical and horizontal components of synthetic seismograms were generated, which contain both the up-going P- and S-wave obtained by using the ray tracing method as seen from Fig. 7. The model parameters for the synthetic seismic are illustrated in Table 5. The VSP offset is 500 m, 321 geophones are located at a range from 400 to 2000 m with 5 m interval and 3 s time duration and a 0.5 ms sampling interval. Note that the significant disadvantages of scalar wave separation with the single component is the loss of the information of seismic events for another component.

Figs. 8 and 9 are the results obtained by using the vector wave separation with an accurate initial value and with an initial value deviation of 50%, respectively. From Fig. 8, one can see that with an accurate initial value one can get the satisfactory result and the interference wave is not visible throughout the record section. From Fig. 9, one can see that the polarization results have been influenced by the initial value deviation of 50%, and there are some interference waves on the crossing of reflections. However, the results still show a great improvement over the original data.

Table 5. Model parameters.

Depth (m)	Velocity of P (m/s)	Velocity of S (m/s)
600	1000	577
740	1300	750
890	1500	866
1040	1800	1039
1180	2000	1154
1370	2300	1327
1545	2500	1443
1710	2700	1558
1890	3000	1932
2000	3500	2020

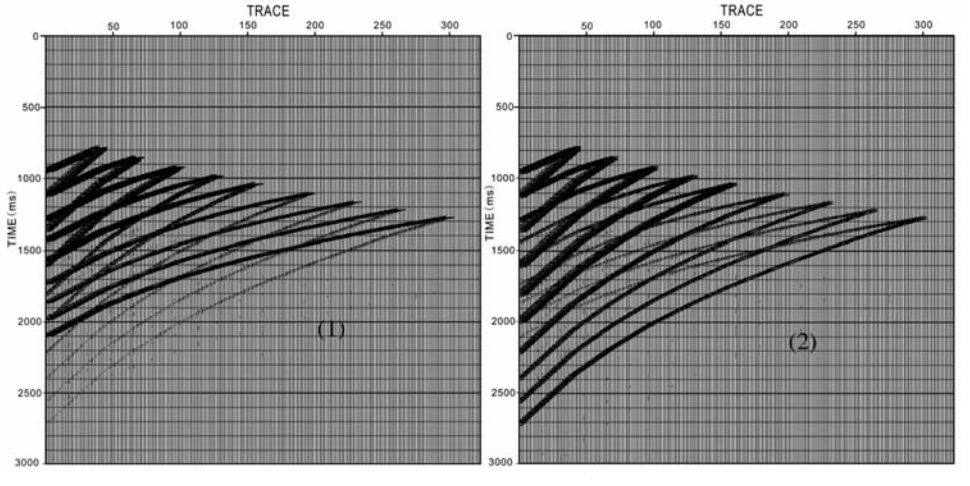

Fig. 7. Synthetic VSP up-going seismograms. (1) Z-component; (2) HP-component.

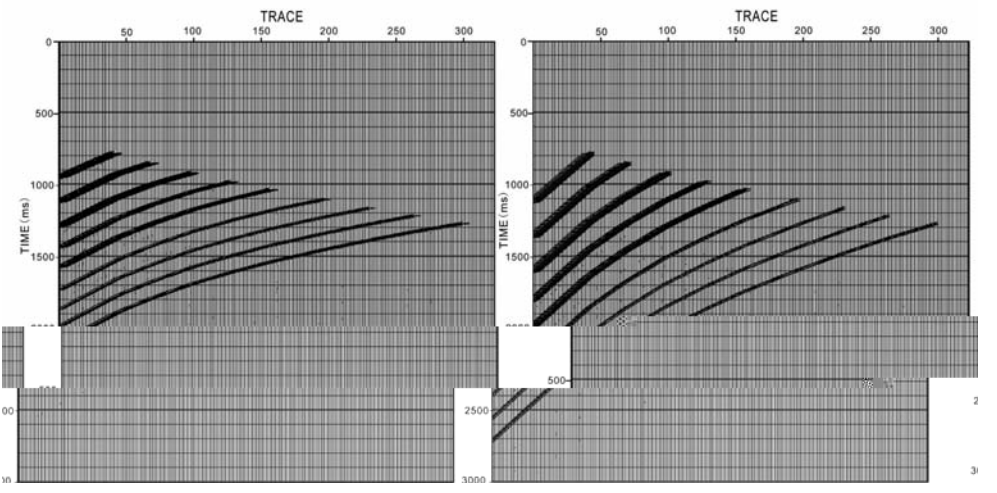

Fig. 8. Synthetic VSP up-going wave separation with the accurate initial value. (1) P-component; (2) S-component.

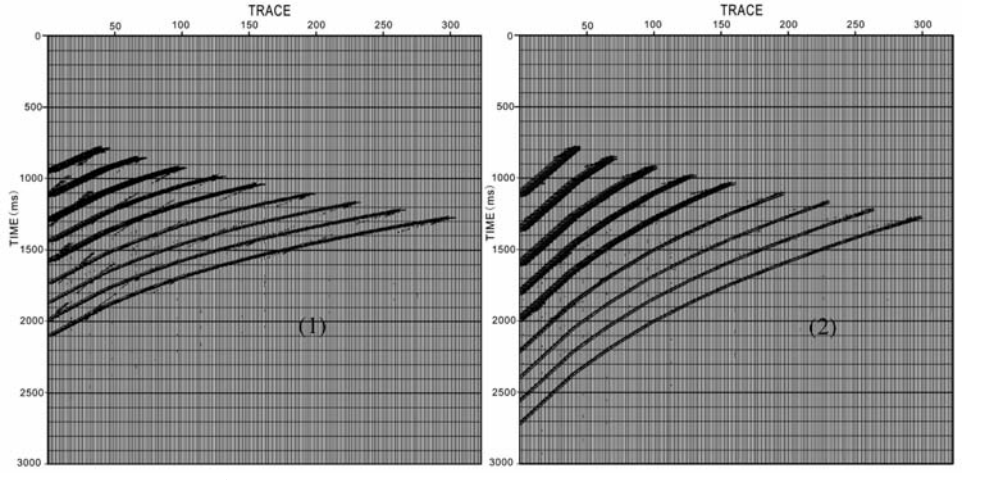

Fig. 9. Synthetic VSP up-going wave separation with an initial value deviation of 50%. (1) P-component; (2) S-component.

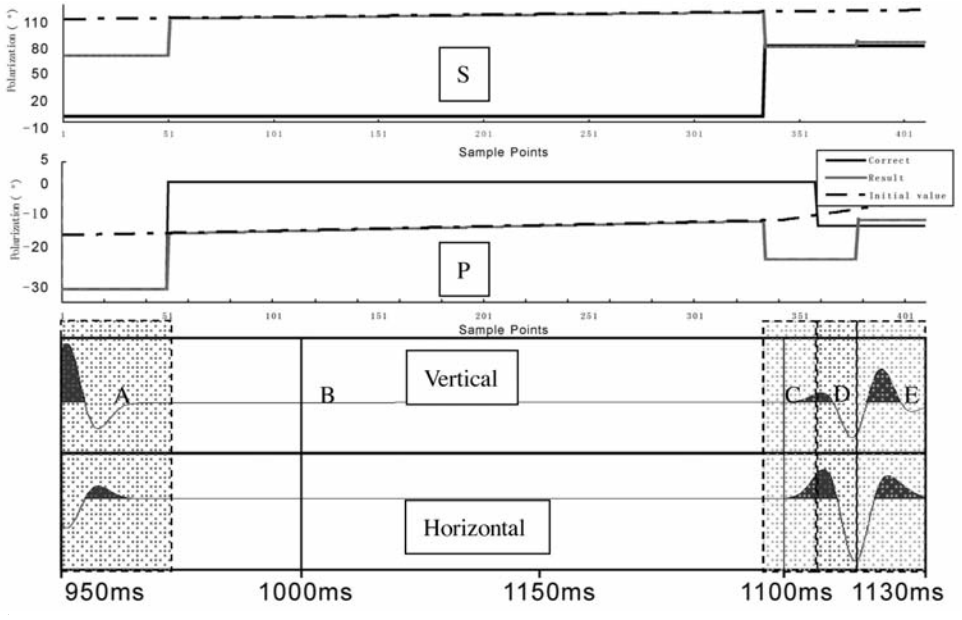

Fig. 10. The performance of the polarization method dealing with different situations in synthetic test (50% initial value deviation).
A. single wave field of P-wave; B. blank; C. single wave field of S-wave; D. mixed wave field NO.1; E. mixed wave field.

We evaluated the performance of the method for dealing with different situations in practical use. The first trace and a time window between the 950 ms and 1130 ms t of synthetic seismograms data mentioned above is chosen for analysis. In Fig. 10, the top two graphs are the polarization characteristic analysis curves, and the bottom two are the vertical and horizontal component seismograms. In the top two graphs, the black solid, black dashed and grey solid lines indicate the correct polarization angle, the initial value and the polarization characteristic result, respectively. The initial values are an oblique line obtained by the linear interpolation of the ray tracing results. We then divide this synthetic multi-component array data into five different situations for specific analysis.

A: A single event wave field of P-waves. Firstly, we identify the seismic event condition with the eigenvalue ratio of the covariance matrix. Then, we calculate the polarization angle of the P-wave from eigenvectors. From

Fig. 10, one can see that the black solid line and the dashed line, which indicate the correct value and the result obtained by using the polarization characteristic algorithm, respectively, coincide with each other. There are some deviations between the correct value and the calculated result for the S-wave. This is because the polarization of the S-wave is assumed to be orthogonal to that of the P-wave. Since the S-wave is not contained in this part, the deviation of the S-wave does not affect the following process at all.

B: Blank wave field, the algorithm will skip this part, so that the polarization results are equal to the initial value.

C: Single event wave field of the S-wave, analogue with part A.

D: Mixed event wave field No.1. since the S-wave is dominated in part D and the eigenvalue ratio of the covariance is less than the threshold value, the event condition of the time window is identified as a single event. So, the algorithm deals with this part the same as part A and part C. The resulting error of P-wave has little affect on the following process since there is little energy of P-wave in part D.

E: Mixed event wave field No.2. In this part, the quasi-Newton optimal algorithm is used. With an initial value deviation of 50%, the error is 1.7° for the P-wave and is 3.7° for the S-wave. Compared with the initial value, the result has been largely improved in accuracy.

Practical seismic test

In this section, we test the performance of the method in a practical seismic application. The VSP data set consists of 1691.11 m offset, 3 s time duration, and 1 ms of sampling interval. 199 geophones in the vertical array are equally spaced within a 10 m interval.

Fig. 11 shows the vertical and horizontal component up-going wave field seismograms after pre-processing of up and down going waves separation, which are separated by using the median and FK filter.

Fig. 12 shows the result of wave field separation obtained by the conventional VSP polarization characteristic method. The conventional method aims to makes a down-going S and a up-going P together into a PP component seismogram, and a down-going P and a up-going S into a PS component. From Fig. 12 one can see that P- and S-waves are not completely separated. This indicates that the conventional method cannot meet the requirement of the polarization characteristic in a practical use.

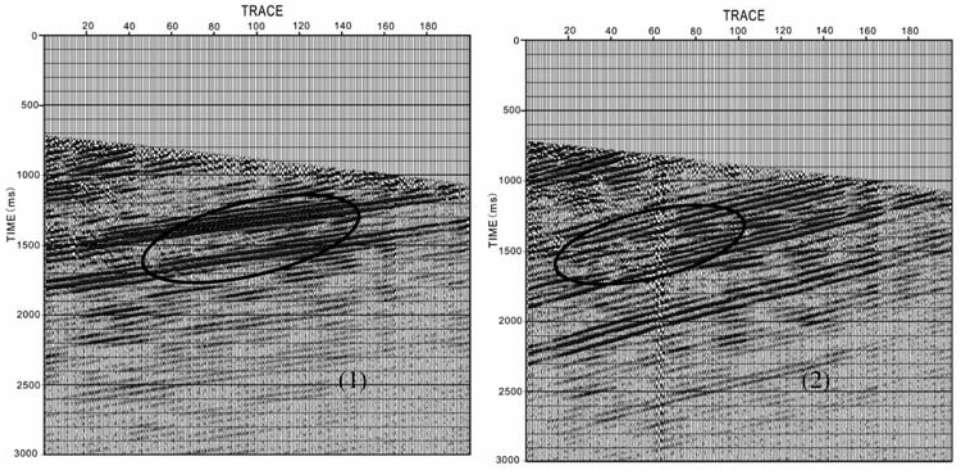

Fig. 11. VSP up-going seismogram. (1) vertical component (Z); (2) horizontal component (HP).

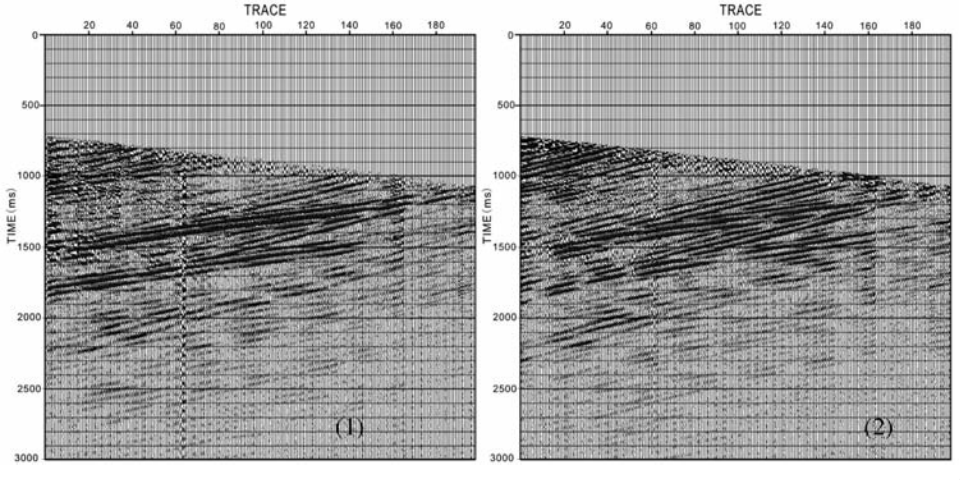

Fig. 12. VSP up-going polarization result with conventional method.
(1) PP-component; (2) PS-component.

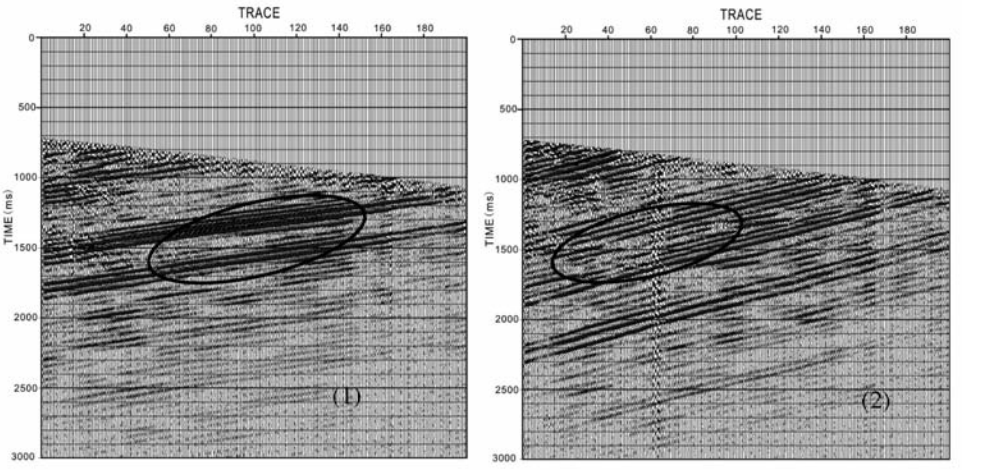

Fig. 13. VSP up-going vector wave separation result with our new time-varying polarization characteristic method. (1) P-component; (2) S-component.

Fig. 13 shows the result of the vector wave separation obtained by using the method developed in this paper. One can see that most of interference waves have been drastically attenuated except for some relatively strong events. From the circle marked on Figs. 11 and 13, a local comparison graph is shown in Fig. 14. The main improvement of B and D as shown in Fig. 14 is that the discontinuity of events caused by interference wave at the crossing of reflections has been significantly attenuated. Moreover, the P- and S-components are not only the result of wave separation, but the result of vector wave synthetic from scalar wave field.

Practical test result indicates that this method can achieve vector wave separation. Although some interference waves exist, most of them are attenuated, and the scalar wave field synthesize successfully to the vector wave field. Compared to the conventional method, the new method is more effective.

CONCLUSION

In this paper, we developed a new method for carrying out the VSP vector wave field separation from multi-component array data set by using the VSP velocity model, covariance matrix analysis and quasi-Newton optimal algorithm. The method can be used for solving many difficult problems associated with wave separation and vector wave synthesize for VSP processing.

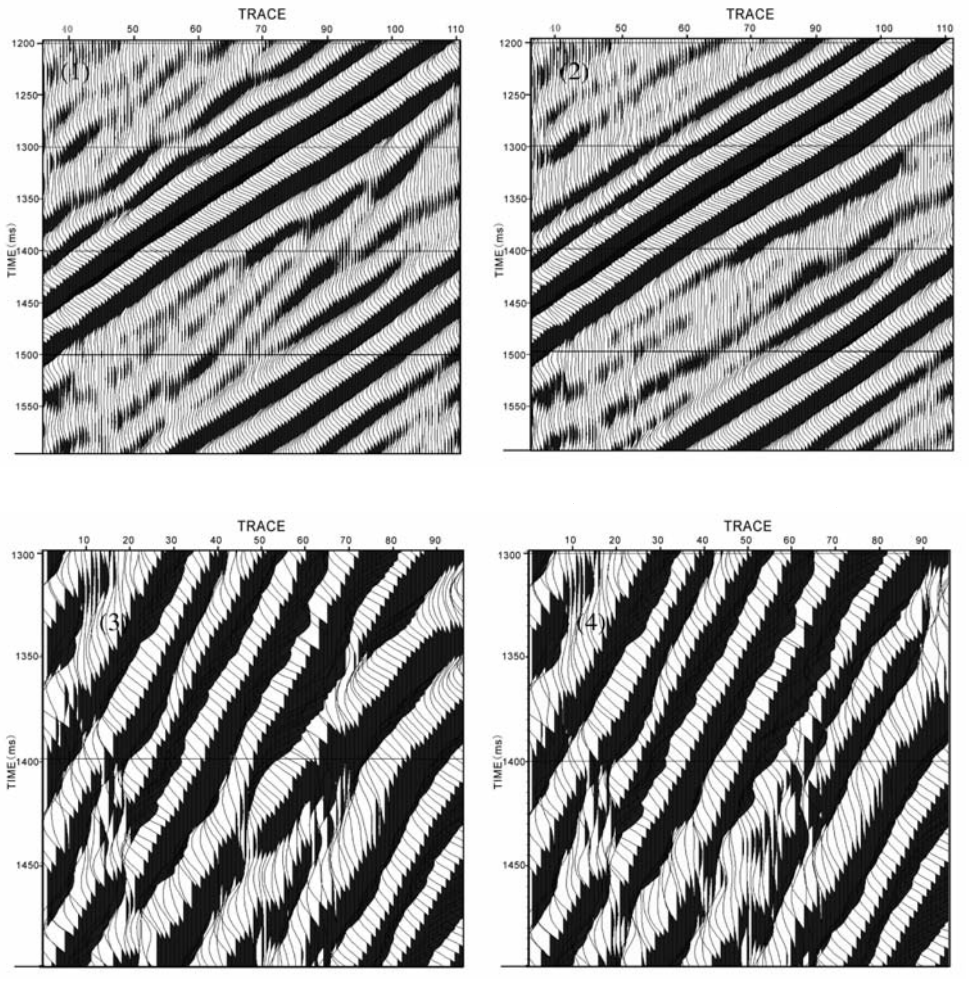

Fig. 14. Local comparison of wave separation result.
(1) Z-component; (2) P-component; (3) HP-component; (4) S-component.

This method also has more elastic advantages, such as it can accommodate more complex situations where the random noise exists and it is not subject to a velocity model. Consequently, with this method, one can separate P- and S-waves from mixed wave fields and synthesize vector wave fields. Moreover, one of the important improvements of this method is its ability to provide an applicable polarization characteristic method and the solutions of many unique problems confronted by VSP processing and interpretation. Numerical analysis show that the method is reliable and stable. And it can be easily extended to other borehole seismic application, such as walk-away and cross-well seismic.

REFERENCES

Cho, W.H. and Spencer, T.W., 1992. Estimation of polarization and slowness in mixed wave field. Geophysics, 57: 805-814.

Cui, J., 1994. A new synthetic method for VSP three-component data. OGP, 29: 368-375.

De Franco, R. and Musacchio, G., 2001. Polarization filter with singular value decomposition. Geophysics, 66: 932-938.

Hardage, B.A., 1983. Vertical Seismic Profiling, Part A: Principles. Geophysical Press, London.

Jackson, G.M., Mason, I.M. and Greenhalgh, S.A., 1991. Principal component transforms of triaxial recording by singular value decomposition. Geophysics, 56: 528-533.

Lilly, J.M. and Park, J., 1995. Multiwavelet spectral and polarization analyses of seismic records. Geophys. J. Internat., 122: 1001-1021.

Vernon III, P.J., 1987. Frequency-dependent polarization analysis of high-frequency seismograms. J. Geophys. Res., 92: 12664-12674.

Reading, A.M., Mao, W. and Gubbins, D., 2001. Polarization filtering for automatic picking of seismic data and improved converted phase detection. Geophys. J. Internat., 147: 227-234.

Samson, J.C., 1983. The spectral matrix, eigenvalues, and principal components in the analysis of multichannel geopysical data. Ann. Geophys., 1: 115-119.